Article

Evaluation of Corrosion Potential Stability of Stainless Steels in Dilute Electrolyte Solution for Application to a Quasi-Reference Electrode Used in Electrochemical Sensing System

Kyosuke Sawada [1],* , Shinji Okazaki [1] , Tatsuki Inaba [2], Motohiro Sakuma [2] and Koichi Azuma [2]

[1] Graduate School of Engineering, Yokohama National University, Tokiwadai 79-5, Hodogaya-ku, Yokohama City 240-8501, Kanagawa, Japan; okazaki-shinji-yp@ynu.ac.jp
[2] R&D, Aichi Tokei Denki. Co., Ltd., Chitose 1-2-70, Atsuta-ku, Nagoya City 456-8691, Aichi, Japan; ta-inaba@inet1.aichitokei.co.jp (T.I.); mo-sakuma@inet1.aichitokei.co.jp (M.S.); ko-azuma@inet1.aichitokei.co.jp (K.A.)
* Correspondence: sawada-kyosuke-ft@ynu.jp

Abstract: To evaluate the long term corrosion potential stability of stainless steel (SS) in environmental water, the corrosion potential of SUS304, SUS316, SUS316L, and SUS430 was measured for 1 week in a solution of 0.9 mM $NaHCO_3$ and 0.5 mM $CaCl_2$, referred to as "sub-tap water." The potential of the SSs upon initial immersion in sub-tap water was approximately 10 times less stable than the potentials of Fe and Cu. However, as immersion continued, the stability of the corrosion potential of the SS improved and became equivalent to those of Fe and Cu. The stability could be manipulated by pretreatment (pre-immersion) before samples were immersed in sub-tap water. The stability was increased by pre-immersion in an acidic solution but was reduced by a passivation treatment. The formation of iron oxides on the SS surface stabilized the potential, whereas surface enrichment with Cr led to instability. This behavior can also be inferred from a comparison of the polarization curves, where the passive current after the passivation treatment was the largest. This result is also speculatively attributed to the corrosion potential in sub-tap water decreasing over time after the passivation treatment. The charge transfer resistance likely contributes significantly to the potential stability, as indicated by an equivalent circuit analysis based on electrochemical impedance spectroscopy. The results showed that, when stabilizing the corrosion potential of SS, there is no need to reduce the charge transfer resistance as with existing reference electrodes. Stability is achieved when the surface thickness is such that the pseudo-capacitance in a dilute solution is less than $10\ \mu F\ s^{\alpha-1} cm^{-2}$ and potential stability does not influence a few changes in the CPE_1 value after potential stability is achieved. The results of this study show that SS can be used as a quasi-reference electrode material. We expect the findings presented herein to strongly affect the development of electrochemical sensors that can be easily used in long term continuous measurements and in situ applications.

Keywords: stainless steel electrode; open circuit potential measurement; quasi-reference electrode; stability of corrosion potential; equivalent circuit

1. Introduction

Electrochemical sensors continue to be developed because of advantages such as ease of manufacture, low cost, and short response time [1–4]. Potential measurements are among the easiest electrochemical measurement techniques that can be conducted using these sensors, and the obtained potential can be used to estimate the corrosion state of

metals and to quantitatively detect target substances. These superior features have led to the widespread interest in potential measurements in applications ranging from chemical substance monitoring in industrial processes to medical applications and basic research on metals [5–10]. In addition, with the remarkable development of the Internet of Things and artificial intelligence technologies in recent years, electrochemical monitoring is expected to be applied in an even wider range of fields, such as environmental monitoring and quality control.

A reference electrode (RE) that serves as a standard for potential is critical for electrochemical measurements, such as potential measurements; currently, the silver–silver chloride (Ag/AgCl) electrode and saturated calomel electrode (SCE) are widely used as REs. However, these REs have drawbacks, including potential drift over time because of liquid junction potential differences and contamination of the internal liquid, as well as the possibility of introducing contaminants into the measurement system [11]. In addition, these REs have structural or use limitations, such as instability in high-temperature and high-pressure environments, difficulty being made compact and durable, and requiring frequent maintenance [11–13]. Because of these drawbacks, applying REs to in situ and continuous industrial process monitoring is difficult.

There have been attempts to develop new REs that overcome these drawbacks. However, if they are used in pH sensors, the potential drift must be kept within 5.9 mV to keep the pH error below 0.1. On the other hand, if it is to be applied to continuous measurement of metals, the potential drift must be kept within 10 mV/day [14].

Studies on all-solid-state Ag/AgCl electrodes are part of broader research aimed at developing new REs that overcome the drawbacks of conventional REs. One example is the use of screen-printing technology. Screen-printed REs are highly reliable because they exhibit a stable equilibrium potential such as conventional REs; they have also been reported to be easily manufactured, compact, and inexpensive [13,15–17]. However, potential measurements using these all-solid-state REs tend to become unstable when the ionic crystalline film deposited onto the substrate to maintain the equilibrium potential deteriorates, necessitating replacement of the entire electrode. Hence, no REs can be used continuously for an extended period without maintenance and without contaminating the measurement system.

Quasi-reference electrodes (QREs) are often used to avoid the problems associated with conventional REs. QREs do not have a specific potential; the potential can change when a QRE is immersed in different solutions even though the QRE is the same material. Therefore, a QRE cannot be used for electrochemical measurements in which the composition of the solution changes substantially during the measurement [11]. However, QREs are considered to be effective reference electrodes when limited to specific applications. Therefore, researchers have attempted to use QREs in place of REs as sensing materials for electrochemical analysis and potentiometric measurements [11,18–21].

Little research has been conducted on small and simple-structure QREs that function stably in environments where the redox concentration is low, such as environmental water or tap water. Although Ag/AgCl QREs are highly functional and convenient, they have a complex structure designed to slow the dissolution of AgCl [22]. QREs that use organic compounds or carbon membranes have been evaluated in ionic liquids and organic solvents, and potential stability tests in aqueous solvents have also been conducted in systems with high concentrations of redox species [11,19,22]. We speculate that the realization of a simple QRE that can function even in solutions with low redox concentration will broaden the range of applications for electrochemical sensors.

Stainless steel (SS) reacts with water and dissolved O_2 forming a stable oxide film. Because of this characteristic, SS is used in various applications as a corrosion-resistant

metal. In addition, under specific conditions where a stable film can be maintained for an extended period, the corrosion potential of SS is expected to be highly stable. Because the film is strongly influenced by the environment, extensive research has been conducted on the formation mechanism and composition [23–26]. However, there have been few reports on the stability of the corrosion potential of SS. Moreover, to the best of the author's knowledge, there have been no studies conducted on using stainless steel as a reference electrode (Table 1).

Table 1. Comparison of QRE properties with previous report.

Materials	Operating Environment	Ref.
Pt/Polypyrrole Film	Acetonitrile, Electrolyte (0.1 M)	[11]
Pt/poly(*N*-ferrocenylmethyl-*N*-allylimidazolium bromide)	acetonitrile and ionic liquid solutions	[19]
Porous carbon	Acidic and neutral solutions (1 M)	[21]
Stainless steel	Dilute solution	This work

In this report, the corrosion potential of SS in simulated tap water was evaluated and compared with those of other practical metals, Fe and Cu. The work here focuses primarily on the stability of the corrosion potential of the metals in dilute solutions that simulate commonly used environments and how to evaluate the stability. In addition, electrochemical impedance spectroscopy (EIS) and polarization tests were performed on the SS to evaluate the relationship among the reaction on the electrode, the surface conditions, and the stability of the corrosion potential.

2. Principle

In order to demonstrate the potential behaviors of the SUS316L electrode, the operating principle in tap water is represented in Figure 1. The corrosion potential of the SS electrode is based on mixed potential theory, as illustrated in Figure 1. The surface of SS is generally covered with protective thin oxide films. Therefore, the anodic reactions are extremely slow reactions associated with the dissolution of metal and the protective surface film composed of metal oxides (curve a). Moreover, because SS is self-passivated in tap water, a small anodic current called the passivation current, which regenerates metal oxides and keeps passive films constant, continuously flows. This current is balanced with the cathodic current (curve b), which generally corresponds to the reduction reaction of dissolved oxygen (DO) in solution without any deaeration treatment. If the immersion environment of the SS is stable, the cathodic reaction rate can be considered constant. However, if the reaction related to the passivation changes due to a change in the surface state of the SS or the presence of influential compounds in the environment, a shift in the anodic current curve can occur. As a result, the balance between the anodic current and the cathodic current shifts, and the potential changes.

The purpose of this study is to find a method for treating SS electrodes that will form a protective oxide film without causing even slight changes in composition in tap water, thereby minimizing the shift in the anodic curve and providing a stable and constant potential in tap water.
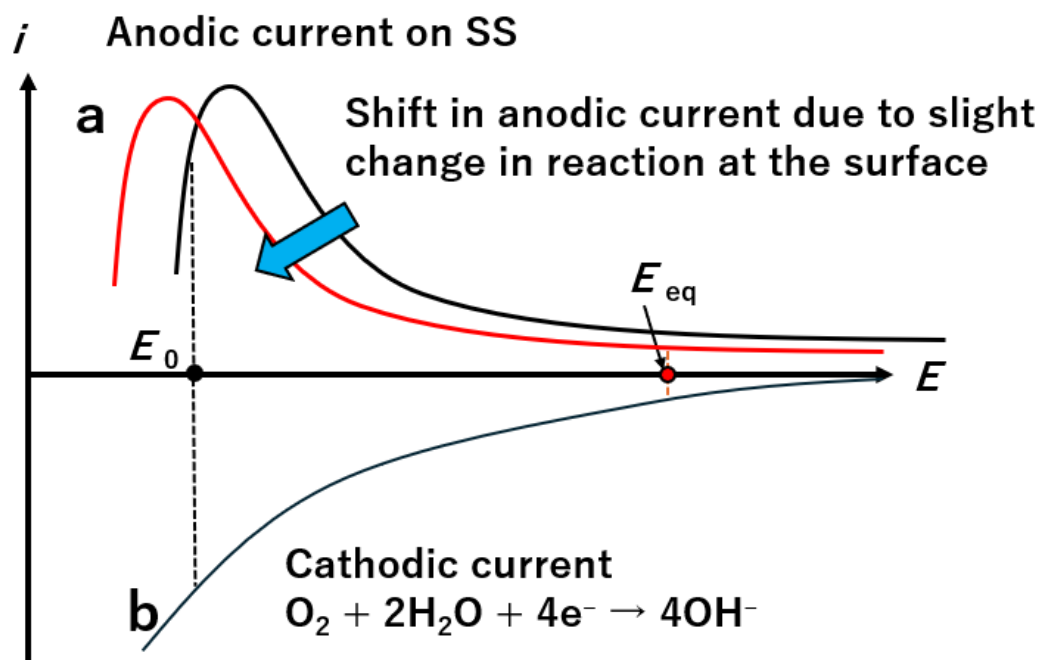
Figure 1. Schematic diagram showing the instability of the corrosion potential of SS in tap water based on the mixed potential theory.

3. Experimental Section

3.1. Materials

SUS304, SUS316, SUS316L, and SUS430 were used as electrode materials. All metals were rods with a diameter of 6 mm; their compositions are shown in Table 2. These rods were fixed and covered in glass tubes with epoxy resin (Struers, Specific Cold Mounting Resin, Copenhagen, Denmark) and processed such that only the end faces were exposed and in contact with the liquid. The SS electrodes were wet-polished with emery paper up to grit 1200 and then washed with ethanol and pure water; the liquid-contacting surface was thoroughly dried using a blower. The electrodes were then left in air for ~1 day before being subjected to the pretreatment and immersion test described in Section 3.2. In addition to the above SS, an Fe (carbon steel: SS400) rod and a Cu (99.9%) rod were also processed in the same manner and used for comparison of the corrosion potential stability.

Table 2. Chemical composition of stainless steels investigated in the present study.

Sample	Chemical Composition [wt%]								
	C	Si	Mn	P	S	Cr	Ni	Mo	Co
SUS304	0.07	0.48	1.87	0.031	0.023	18.47	8.03	-	0.26
SUS316	0.05	0.35	1.42	0.037	0.024	16.96	10.06	2.05	-
SUS316L	0.02	0.49	0.83	0.031	0.001	17.45	12.09	2.03	0.30
SUS430	0.04	0.27	0.27	0.028	0.002	16.18	-	-	-

3.2. Surface Treatment for Stainless Steel

As a pretreatment, an immersion treatment before immersion in the test solution (referred to here as treatment pre-immersion) was carried out for the SS electrodes prepared as described in Section 3.1. The treatment pre-immersion was conducted to evaluate the effect of differences in the surface state due to pretreatment on the potential stability of the electrodes. Solutions of 1 wt% sulfuric acid (H_2SO_4) and 1 wt% sodium carbonate were separately prepared as the immersion solutions for the pretreatment, and SS electrodes were immersed in these solutions at room temperature for 5 min.

Nitric acid (HNO_3) solutions with concentrations of 12 wt%, 20 wt%, and 30 wt% were prepared, and the SS samples were immersed in them at room temperature for 60 min to investigate the effects of acid concentration and temperature. Samples were also immersed in 30 wt% HNO_3 at room temperature for 30 min and in 30 wt% HNO_3 at 70 °C for 30 min.

3.3. Stability Testing of Corrosion Potential

Corrosion potential (open-circuit potential, OCP) measurements were performed using a sample metal electrode as the working electrode (WE) and an Ag/AgCl electrode (3.33 M, +0.206 V vs. standard hydrogen electrode (SHE)) as the RE to compare the short-term and long term potential stability of the samples. The test solution was a mixture of 0.9 mM $NaHCO_3$ and 0.5 mM $CaCl_2$ (we refer to this solution as sub-tap water) at room temperature (25 °C), normal pressure, and in air; this solution was used to simulate tap water. The pH of the solution was 7.13 ± 0.08, and no buffer solution was added. The OCP measurements were carried out using a high-input-impedance electrometer built into an HZ-7000 Potentio galvanometer (Meiden Hokuto, Megro-ku, Tokyo, abbreviation if available, Japan). The measurements were conducted three times each. While there were differences in the initial potentials even under the same conditions, the potential behaviors were similar (the standard deviation of the steepest gradient in the data from the first 2 h of immersion was 3 mV/h). When evaluating the long term corrosion potential stability, sub-tap water was not added or replaced, and the container containing the sample and solution was left at room temperature (25 °C) with a lid on to prevent the contents from evaporating. Because the measurements were conducted over a long period of time and there was a hole in the lid, the experiment was conducted under the assumption that the oxygen concentration in the solution was constant.

3.4. Electrochemical Analysis

EIS measurements and polarization tests were carried out to clarify the correlation between the surface state and corrosion potential stability. The tests were performed in a three-electrode cell using an HZ-7000 (Meiden Hokuto). The SS samples were used as the WE, an Ag/AgCl electrode (3.33 M, +0.206 V vs. SHE) was used as the RE, and Au was used as the counter electrode (CE).

The EIS measurements were performed by first measuring the OCP of the sample for 30 s and then applying an AC voltage of 10 mV in the frequency range from 10 kHz to 0.1 Hz. The analysis of the EIS measurement results, including equivalent circuit analysis, was performed using the Levenberg–Marquardt method in the EIS software (EIS 1.4.1) provided with the HZ-7000. This measurement was also performed in sub-tap water at room temperature.

The polarization tests were performed under various conditions depending on the observations of the measured samples. To confirm their basic corrosion resistance, the samples were polarized at a constant potential of -0.65 V vs. Ag/AgCl for 10 min in 5 wt% H_2SO_4 solution degassed with N_2 for 30 min according to the JIS standard; they were then left at the corrosion potential for 10 min, after which the samples were polarized from the corrosion potential to $+1.2$ V vs. Ag/AgCl at a voltage application rate of 20 mV/min [27]. To evaluate the effect of pre-immersion of the SS samples in sub-tap water, samples were polarized in sub-tap water under open atmosphere for 10 cycles at various sweep rates from -0.7 V vs. Ag/AgCl to $+0.8$ V vs. Ag/AgCl.

4. Results and Discussion

4.1. Potential Stability of Stainless Steels Without Pre-Immersion

Figure 2 shows the time-dependent change in the corrosion potential and potential drift for each sample after it was immersed for 7 days in sub-tap water. For all of the electrode materials, the initial large potential fluctuation subsided approximately 2–3 days after immersion. The potential gradient (drift) for all of the SS samples was 6 mV/day when the immersion time was 5 days or less; however, the drift after 3 days of immersion was 7.0 mV/day for Fe and 1.2 mV/day for Cu. As a result of this, it is necessary to immerse SS for 5 days or more to stabilize the potential. When the materials are compared on the basis of their long term potential stability, Cu and Fe were superior to SS. These results suggest that relatively simple materials are superior to an alloy with excellent corrosion resistance.
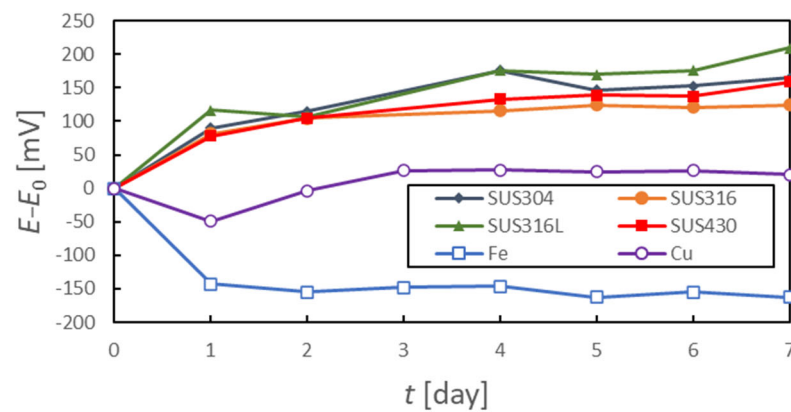
(**a**)
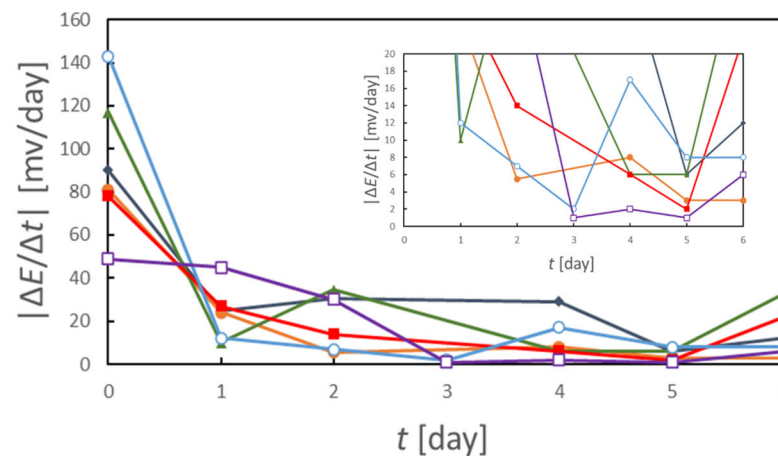
(**b**)

Figure 2. Result of 7 days of intermittent potential measurements: (**a**) potential changes relative to the initial potential and (**b**) the rate of change of potential difference.

In order to evaluate the short-term potential stability, the fluctuations of OCP were extracted. Figure 3a,g show the OCP measurement result (measurement intervals of 1 s) for the electrodes that were only polished, immediately after they were immersed in sub-tap water for 24 h (Figure 3a) and after they were immersed for 168–192 h (Figure 3g). The Y-coordinate represents the potential difference between the corrosion potential E at time t and the corrosion potential E_0 at $t = 0$ immediately after each electrode was immersed in sub-tap water. Figure 3b–f,h–l show the time-dependent changes of the standard deviation

of the potential, which was used as an index of potential stability; the standard deviation was calculated every 30 s using the boxcar method.
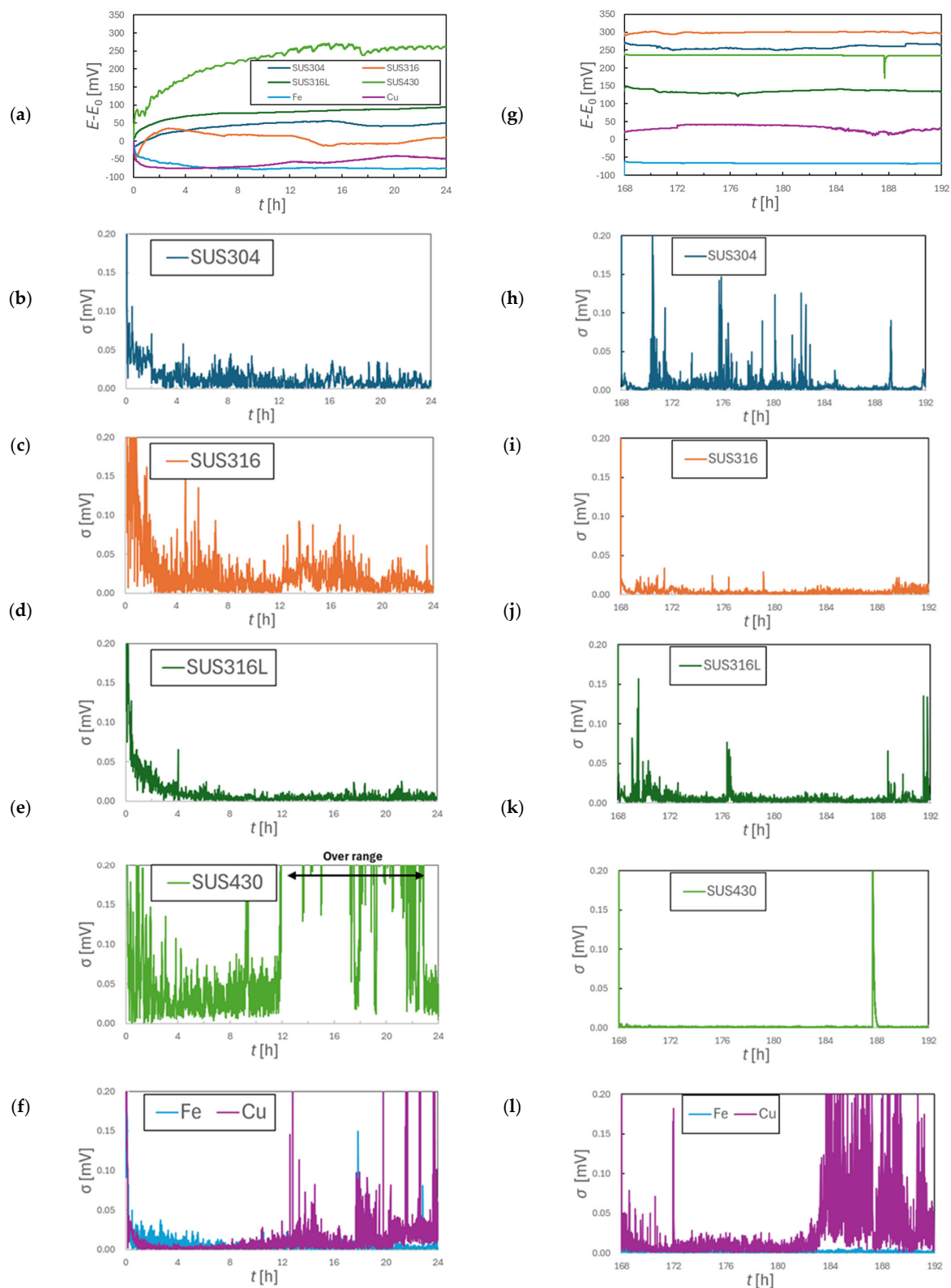
Figure 3. Potential changes (**a**) from the initial potential upon immersion to that 24 h after immersion and (**g**) from the potential 168 h after immersion to that 192 h after immersion. Standard deviation of the potential (**b**–**f**) from the point of immersion to 24 h after immersion and (**h**–**l**) from 168 h to 192 h after immersion. The standard deviation was calculated every 30 s.

The Fe electrode showed smaller potential fluctuations and a more stable corrosion potential than the SS and Cu electrodes, which exhibited excellent corrosion resistance (Figure 3a). In particular, Fe maintained a constant potential after 6 h of immersion in sub-tap water. The Cu electrode continued to show a small potential fluctuation for the first 4 h of immersion; however, the potential fluctuation range for the Fe electrode was the smallest after 6 h. The standard deviation, σ, of the potential fluctuation for Fe at the beginning of immersion also showed little change (Figure 3f). A change in standard deviation can be one indicator of potential stability. All of the SS samples showed large potential fluctuations in the early stages of immersion after the electrodes were polished; the potential fluctuations tended to subside between 4 and 8 h (Figure 3a–e).

The potential stability also differed depending on the type of SS investigated. The standard deviation of the potential fluctuations for the austenitic SUS300 series fell below that for Cu after 0–8 h of immersion in sub-tap water. For SUS316L, the potential fluctuations stabilized at 10–20 μV (Figure 3d), the same level as for Fe. These results indicate that, immediately after polishing, materials that are most susceptible to corrosion exhibit stable corrosion potentials earlier on. Thus, in the case of simple metals, the potential tends to be more stable for materials on which the reaction is simple and corrosion is more likely to occur. By contrast, for alloys that form a passivation film, such as SS, higher corrosion resistance leads to slower stabilization of the alloy's corrosion potential.

We found that the standard deviation for all of the SS samples was less than 50 μV for most of the time when they were immersed for 168 h or more in sub-tap water, although the change in potential from the initial stage varied greatly depending on the type of SS (Figure 3h–k). In addition, the pH of sub-tap water was 7.35 ± 0.10 after potential measurement after 7 days of immersion, and it was found that the solution remained neutral during immersion. This shows that the corrosion potential of SS can be stabilized by its continued immersion in a constant environment, at least in neutral solutions. Furthermore, unlike the intermittent measurements over 7 days, the continuous two-hour potential observation revealed that SS exhibited higher potential stability compared to Cu. Although the tendency for SS to be more stable than Cu was observed immediately after immersion during the continuous two-hour measurement, it was also found that SS was less stable than Fe even after seven days of continuous immersion. (Figure 3h–l).

4.2. Potential Stability of SS with Pre-Immersion

To examine the effectiveness of pre-immersion, we measured the corrosion potential of the SS samples in sub-tap water after the samples were immersed in various pretreatment solutions for 5 min. Irrespective of the pre-immersion solution or type of SS, the potential fluctuations tended to decrease as the immersion in sub-tap water was continued for 2 days. The results in Figures 3 and 4 show that the stability of the corrosion potential in sub-tap water can be controlled by pre-immersion. Moreover, it was also found that pre-immersion could shorten the stabilization time from 5 days to about 3 days.

Using the results from Figure 4, we calculated the standard deviation and slope from the second day onward; the results are summarized in Table 3. These results also show that the stability of the corrosion potential can be changed by pre-immersion. Regarding treatment, pre-immersion in H_2SO_4 solution reduced the standard deviation of the potential fluctuations for SS by at least 17% and the drift by at least 63%, except for SUS304; by contrast, pre-immersion in Na_2CO_3 solution only reduced the standard deviation for SUS304 and the drift for SUS316 and SUS316L. Comparing the stability in Table 3, it was found that the 300 series with added nickel was more stable than SUS430. It is believed that the greater corrosion resistance of the material itself affects the stability of the potential.

In addition, we speculate that pre-immersion in an acidic solution stabilizes the corrosion potential in a dilute solution such as environmental water or tap water.
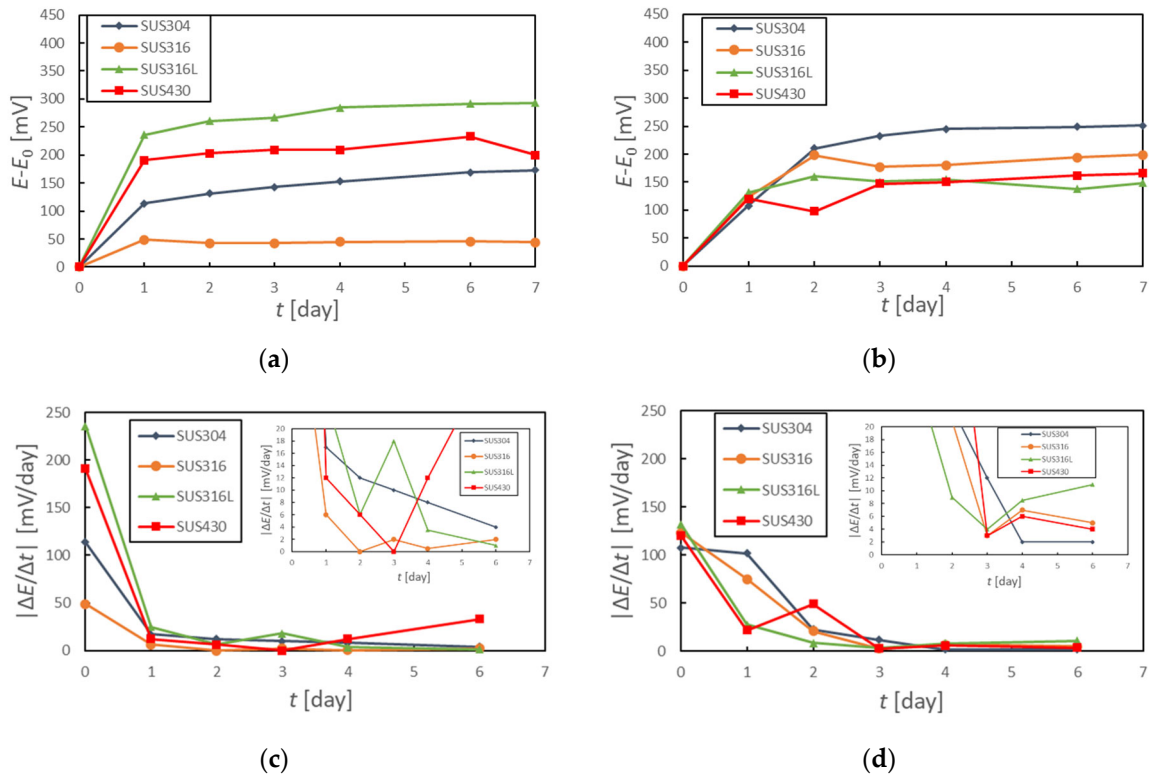

(**a**)

(**b**)

(**c**)

(**d**)

Figure 4. Results of 7 days of intermittent potential measurement after SS electrodes were immersed in (**a**,**c**) 1 wt% H_2SO_4 solution for 5 min and (**b**,**d**) 1% Na_2CO_3 solution for 5 min. Subfigures (**a**,**b**) show potential changes relative to the initial potential; subfigures (**c**,**d**) show the rate of change of the potential difference.

Table 3. Standard deviation of potential σ and potential gradient in sub-tap water from 2 days to 7 days after immersion in H_2SO_4 or Na_2CO_3 solution.

Pre-Immersion	SUS304		SUS316		SUS316L		SUS430	
	σ [mV]	$\|\Delta E/\Delta t\|$ [mV/Day]	σ [mV]	$\|\Delta E/\Delta t\|$ [mV/Day]	σ [mV]	$\|\Delta E/\Delta t\|$ [mV/Day]	σ [mV]	$\|\Delta E/\Delta t\|$ [mV/Day]
N/A	23.1	5.2	8.0	13.7	17.7	17.9	19.4	9.6
1% H_2SO_4	17.6	8.4	1.3	0.4	14.7	6.7	13.0	1.7
1% Na_2CO_3	16.9	7.1	10.4	1.9	8.2	2.9	27.2	11.0

Figure 5 shows the results of measurements of the corrosion potential of the SS samples in sub-tap water after the electrodes were immersed in HNO_3 solutions with different concentrations for 30 min. Even when pre-immersion was carried out in HNO_3 solution, the change in potential was reduced by immersion in sub-tap water for 2 days, irrespective of the HNO_3 concentration. Therefore, the drift and standard deviation were also calculated 2 days after pre-immersion in HNO_3 solution and then immersion in sub-tap water; the results are summarized in Table 4. The results in Table 4 were also calculated in the same way as the results in Table 3. When the SS samples were pre-immersed in HNO_3 solution with a concentration of 12% or greater, the standard deviation and the drift could be reduced compared with those for SS samples not subjected to pre-immersion. However, the fluctuation in corrosion potential every 24 h was greater for treated SS than for untreated SS, and the potential difference was often 10 mV/day when measured starting 2 days after immersion in sub-tap water. These results show that the stability of the corrosion potential

of SS after immersion in a dilute solution can vary greatly depending on the concentration of the acid solution. In addition, pre-immersion for 30 min in a 30 wt% HNO_3 solution heated to 70 °C resulted in a greater potential difference and a standard deviation in sub-tap water than those of the sample without pretreatment in Figure 3 (Figure 5d). This result implies that pre-immersion in a strongly oxidizing solution is disadvantageous from the viewpoint of improving the potential stability.
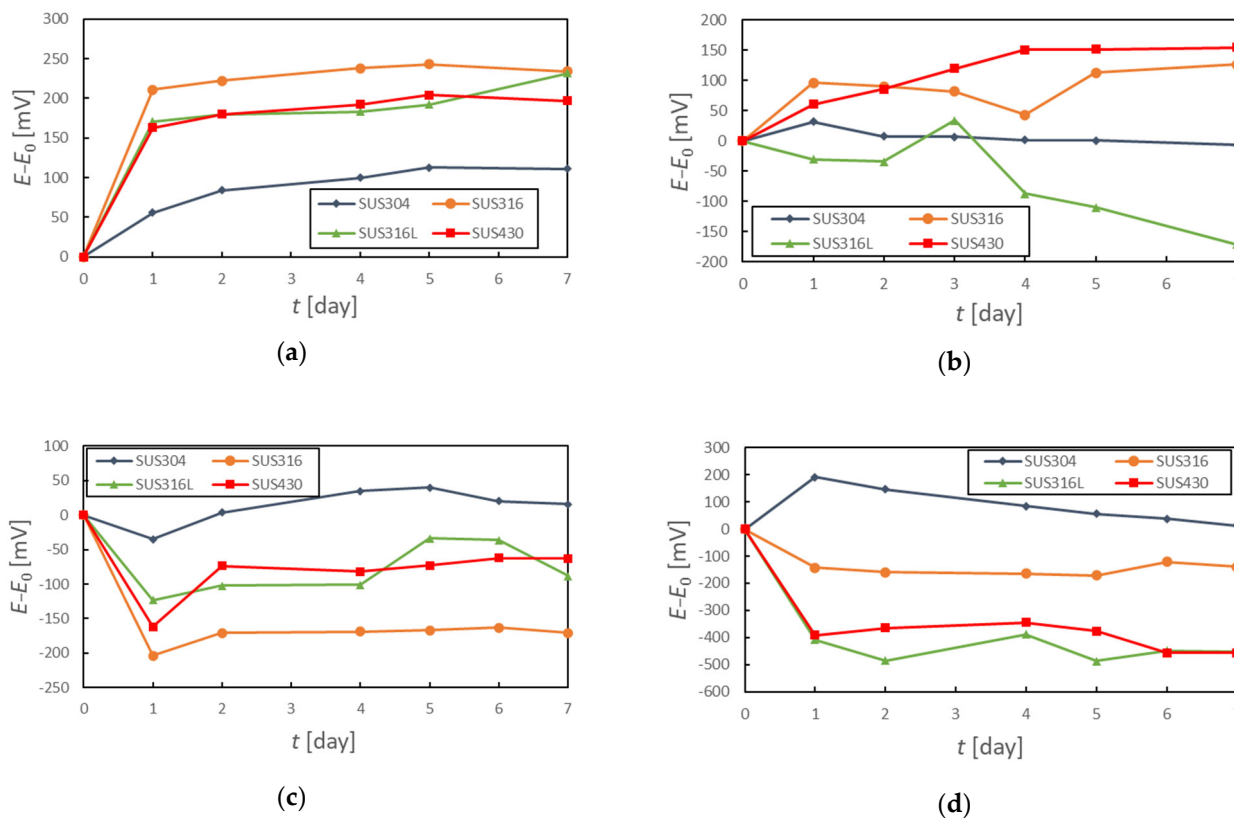

Figure 5. Potential changes for SS electrodes relative to their initial potential in sub-tap water after the electrodes were immersed in an HNO_3 solution with a concentration of (**a**) 12%, (**b**) 20%, or (**c**) 30% at room temperature for 30 min and (**d**) 30% at 70 °C for 30 min.
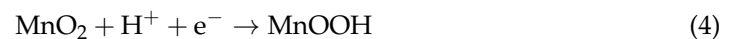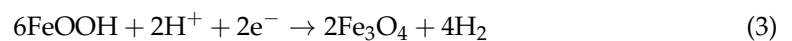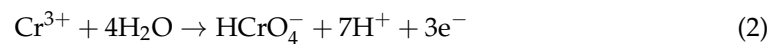
Table 4. Standard deviation of potential σ and potential gradient in sub-tap water from 2 days to 7 days after immersion in HNO_3.

Concentration of HNO$_3$	SUS304		SUS316		SUS316L		SUS430	
	σ [mV]	$|\Delta E/\Delta t|$ [mV/Day]	σ [mV]	$|\Delta E/\Delta t|$ [mV/Day]	σ [mV]	$|\Delta E/\Delta t|$ [mV/Day]	σ [mV]	$|\Delta E/\Delta t|$ [mV/Day]
12% (r.t.)	13.3	5.7	9.0	2.5	24.0	10.3	10.1	3.7
20% (r.t.)	6.0	3.1	32.3	9.5	77.7	34.8	30.0	13.0
30% (r.t.)	14.6	1.9	3.3	0.6	34.4	8.3	8.4	3.1
30% (70 °C)	51.1	26.4	20.7	6.4	39.5	2.9	52.8	22.3

The potential stability decreased after pre-immersion in concentrated HNO_3 solution for 30 min, presumably because the Cr-rich film formed in HNO_3 solution gradually changed into a film with a different composition that was stable in sub-tap water (i.e., an iron–chromium oxide film with a composition ratio similar to that of the bulk). According to Takizawa [28], the ratio of metals present on the surface of SS changes depending on the method of surface treatment. In particular, the ratio of Fe and Cr on the surface of

passivated SS was similar to that in the bulk steel when the SS was polished alone, whereas when passivation was performed with HNO_3 solution after polishing, the ratio of Fe and Cr was reversed, with the Cr concentration increasing to more than twice that in the bulk [28]. In the present study, the corrosion potential of the SS samples in sub-tap water after pre-immersion in 30 wt% HNO_3 solution heated to 70 °C gradually decreased from +200 mV vs. Ag/AgCl or higher. From these results, we inferred that, in the present study, a Cr-rich film was formed on SS samples immersed in concentrated HNO_3 solution; however, with increasing immersion time in sub-tap water, the film changed to one with a lower corrosion resistance and a lower Cr ratio. This result suggests that the potential stability of SS in sub-tap water is greatly affected by the composition of the passivation film on the SS.

The potential fluctuations in the mixed electrode reaction system, which result in long term potential instability, are thought to be caused by an increase or decrease in the reaction rate when chromium oxide in the film dissolves and changes into a different oxide. The potential–pH diagram shows that chromium(III) oxide (Cr_2O_3) is stable in sub-tap water [29]. Yixun et al. [30] have also reported that the ratio of Cr_2O_3 in the film increased when SS was immersed in a high-temperature HNO_3 solution. This observation suggests that, in the present study, the composition ratio of Cr_2O_3 also increased on the film passivated in concentrated HNO_3 solution. However, sub-tap water is a neutral solution containing coexisting chemical species with weak oxidizing power, such as dissolved O_2; the stable chemical species is $Cr(OH)_2^+$ [29]. Because Cr_2O_3 continues to remain on the passivation film after surface treatment [28], it is thought that Cr_2O_3 was in a metastable state even at temperatures below tap water level and did not immediately ionize and dissolve. However, because of changes in the cathodic reaction rate caused by local increases in the O_2 and Cl^- ion concentrations, the stable state of some parts of the surface changes, and parts where Cr dissolution progresses can appear. As the dissolution of Cr_2O_3 accelerates, the concentration gradient between the bulk metal and the metal in the film increases; this process acts as a driving force to promote the supply of metal to the surface, changing the rate of regeneration of the passivation film. Due to the above considerations and the potential–pH diagram, it is believed that the potential stabilizes as the dissolution of chromium via anode reactions (1) and (2) subsides [29,31]. Based on the contents of Section 4.3 described below, not only the cathode reaction, which corresponds to the reduction reaction of DO, but also the iron and manganese reduction reactions (3) and (4) can also be important reactions for making the potential stable [31].

$$2Cr^{3+} + 7H_2O \rightarrow Cr_2O_7^{2-} + 14H^+ + 2e^- \tag{1}$$

$$Cr^{3+} + 4H_2O \rightarrow HCrO_4^- + 7H^+ + 3e^- \tag{2}$$

$$6FeOOH + 2H^+ + 2e^- \rightarrow 2Fe_3O_4 + 4H_2 \tag{3}$$

$$MnO_2 + H^+ + e^- \rightarrow MnOOH \tag{4}$$

4.3. Voltammetric Analysis

Figure 6 shows polarization curves for various SS samples polarized in deaerated 5% H_2SO_4 to confirm the current density when a stable passivation film is formed. Figure 6 shows that SUS316L exhibited the largest passive current density among the investigated SS samples and appeared to exhibit the fastest oxidation reaction, which reinforces and maintains the film. This observation and result of Figure 3 suggest that the regeneration speed of the passivation film on electrodes may strongly affect the stability of their potential.
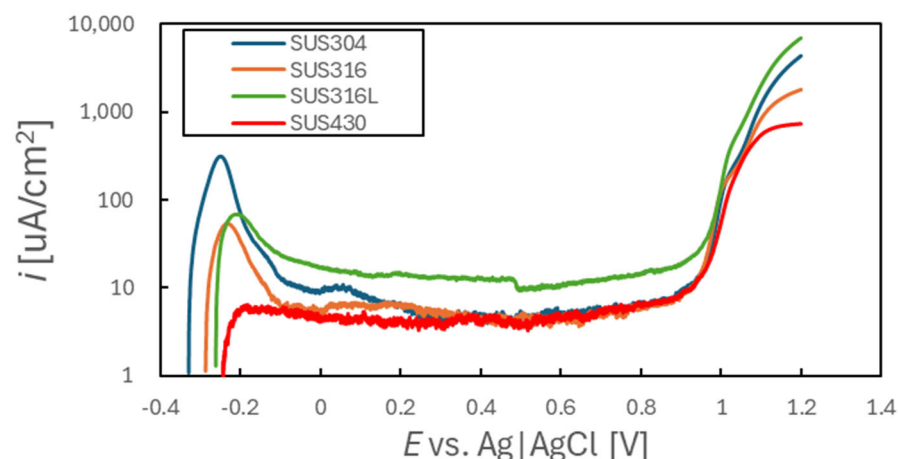
Figure 6. Linear sweep voltammogram for SS in 5 wt% H_2SO_4 solution (scan rate: 20 mV/min).

Figure 7 shows anodic polarization curves for SUS316 polarized in sub-tap water after different pre-immersion treatments. The potential fluctuation decreased with increasing immersion time because the reaction rate on the SS surface gradually slowed as a result of the current density decreasing with increasing cycle number irrespective of the treatment (Figure 7). A comparison of the current densities reveals that it was under 20 $\mu A/cm^2$ for all of the samples from the 1st cycle. It also confirms that a passivation film was formed by immersion in sub-tap water, as evident from the magnitude of this current density being similar to that in the passivated region in Figure 6.

These results also suggest that the film formed in concentrated HNO_3 solution changed composition most rapidly in sub-tap water. They may further indicate poor stability of the passivation film formed in concentrated HNO_3 solution because the current density for the specimen immersed in 30% HNO_3 solution from the 1st to the 10th cycle was greater than that in the passivated region. Notably, however, the composition changed without complete destruction of the film, whose presence was confirmed from the magnitude of the current density in each cycle after the sample was immersed in HNO_3 solution (Figure 7). On the basis of the results presented in Section 4.2, the reaction that occurred on the surface during immersion in HNO_3 solution changed the film from a Cr-rich oxide to a film mainly composed of iron oxides, which is stable in dilute solutions such as tap water. From these results, we considered that if a film with a composition that differs from that of the stable film formed in dilute solutions such as tap water, the reaction leading to a composition change is more likely to occur, making the passive current density more likely to fluctuate and impairing the long term potential stability.

Figure 8 shows polarization curves recorded for SS electrodes in sub-tap water after the electrodes were pre-immersed in 1 wt% H_2SO_4 solution for 5 min. It can be seen that the relationship between the current densities of the SSs changed from the 1st to the 10th cycle. This relationship between the current densities is summarized in Table 5, together with the results for the potential stability after the electrodes were immersed in H_2SO_4 solution (Table 3). Figure 8 suggests that forming a stable film in sub-tap water through pre-immersion is important for improving the corrosion potential stability of SS and that one effective method to form such a film is to clean the surface via acid pickling and weaken the film formed in air. The current density for SUS304, whose drift in sub-tap water after pre-immersion in H_2SO_4 solution was larger than that after polishing alone and whose potential was unstable (Table 3), was still greater than those for the other SS samples even at the 5th cycle in Figure 8b. This result suggests that the reaction on the passivation film of SUS304 continued to occur. By contrast, SUS316, which had the most stable potential, already developed a current density of 10 $\mu A/cm^2$ at -0.2 V vs. Ag/AgCl in the 2nd cycle.
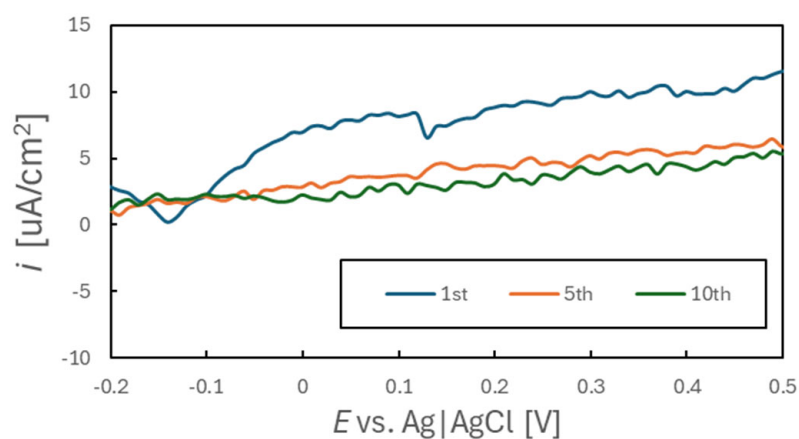
This potential is approximately the corrosion potential of SS observed in the test and is also considered to be the potential at which the SS was passivated [32]. The passivation current corresponds to infinitesimal oxidation reactions of component metals or metal oxides.
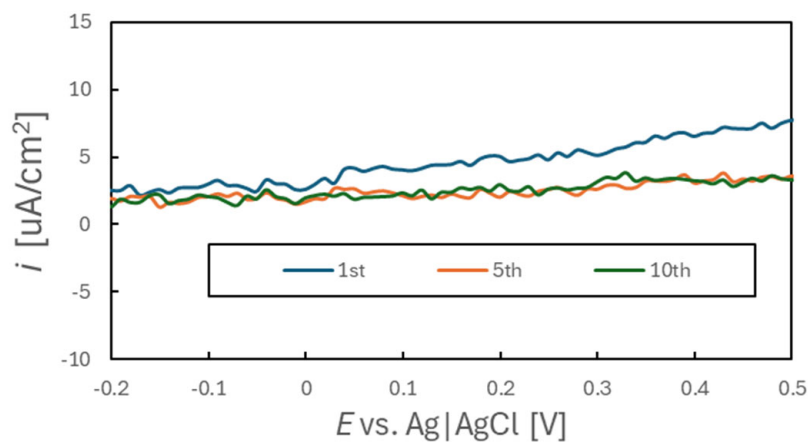
(**a**)
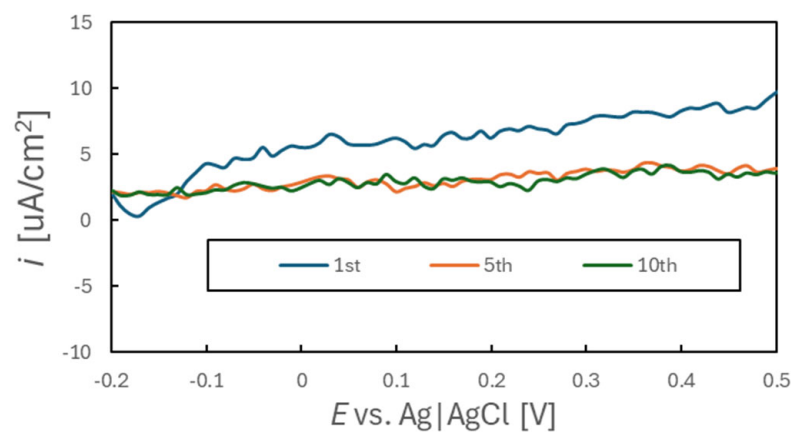
(**b**)

(**c**)

Figure 7. Anodic polarization curves for SUS316 in sub-tap water after pre-immersion that was carried out in different liquids (scan rate: 1 mV/min): (**a**) Only polishing (not implemented pre-immersion treatment), (**b**) after immersion in 25 °C 1% sulfuric acid for 5 min, and (**c**) after immersion in 30% nitric acid heated at 70 °C for 30 min.
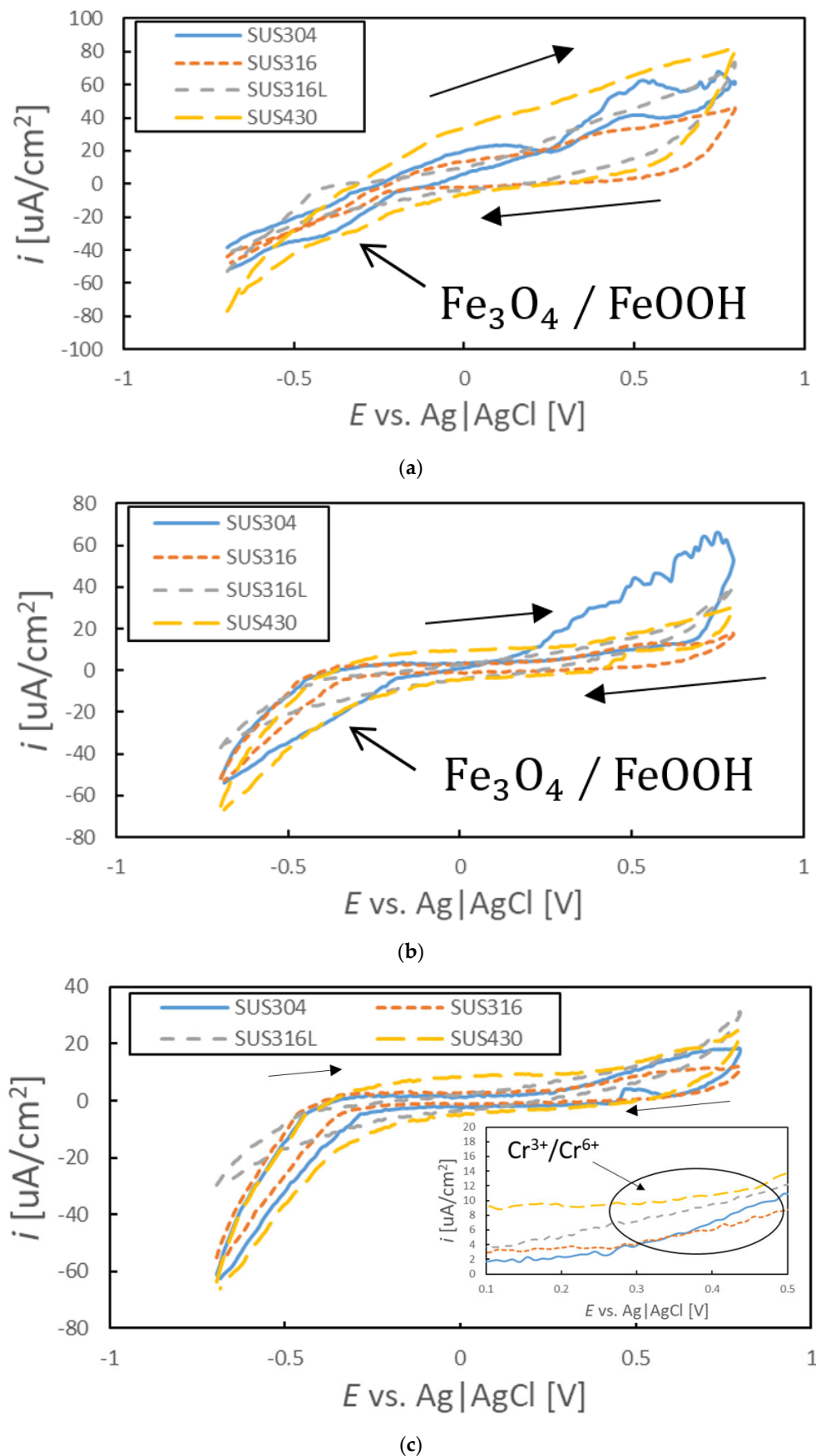
(**a**)

(**b**)

(**c**)

Figure 8. Cyclic voltammogram for SS after immersion in 1 wt% H_2SO_4 solution for 5 min (scan rate: 10 mV/min): (**a**) 1st cycle, (**b**) 5th cycle, and (**c**) 10th cycle.

Table 5. Relationship between current density for passive potential and potential stability (standard deviation of potential) for SS in sub-tap water after immersion in 1 wt% H_2SO_4 solution for 5 min. Current density was calculated as the average from -0.2 V to 0.3 V.

	σ [mV]	Current Density [μAcm^{-2}]		
		Cathode Cycle		
		1st Cycle	5th Cycle	10th Cycle
SUS304	17.6	9.40	3.92	-2.16
SUS316	1.3	-1.32	-0.76	-0.88
SUS316L	14.7	-2.70	-3.45	-2.67
SUS430	13.0	-5.72	-4.63	-4.67

The results also indicate that a lower reaction rate on the electrode surface of a material tends to lead to a more stable corrosion potential. This assertion is supported by the results in Table 5, which show that the smaller the standard deviation and the more stable the potential of a material, the lower the current density during polarization toward the cathode. Specifically, SUS316, which indicated the smallest standard deviation of potential, showed the smallest absolute value of current density and almost constant level through the cycles. In contrast, SUS304 indicated a large current density at the 1st cycle, and the current density considerably changed to reverse the direction of a reaction at the 10th cycle.

We assumed that the passivation film, which is important for maintaining a stable potential in sub-tap water, is mainly composed of iron oxides. In the polarization curves, increasing current density was observed at $+0.3$ V vs. Ag/AgCl during anodic polarization even at the 10th cycle for all of the SS samples in Figure 8c. This peak suggests that Cr dissolution and/or changing reaction (Cr^{3+}/Cr^{6+}) continued to occur, as mentioned by L. Freire et al. [32]. In addition, during cathodic polarization, the peak at -0.3 V vs. Ag/AgCl [32], which we speculatively attributed to Fe_3O_4/FeOOH, disappeared in the 3rd cycle of the SUS316 polarization curves; however, the peak continued to appear beyond the 3rd cycle in the polarization curves for the other SS samples and continued to appear for the longest time (up to the 7th cycle) in the curves for SUS304 (Figure 8a,b). As described in Section 4.2, if a Cr-rich film was present, the potential would be unstable because an iron-oxide-rich film is important for stabilizing the potential.

4.4. EIS Analysis

Figure 9 shows the results of EIS measurements for the electrodes in sub-tap water after they were subjected to each pretreatment. In Figure 9, the results for SUS430 are presented as an example, while the diagrams for other conditions are included in the Supplemental Materials (Figures S1–S3). In the Nyquist diagram, the real part of the impedance Z_{Re} is calculated by subtracting the real part of the impedance at the highest frequency Z_{Re0} from the value obtained at each frequency to compensate for slight differences in solution resistance. Z_{Re0}, which corresponds to the solution resistance, varied by ~10% depending on the sample; however, the magnitude of Z_{Re0} did not affect the corrosion potential, and no correlation was observed between the magnitude of Z_{Re0} and the change in the potential over time.

In the Nyquist diagrams, the magnitude of the imaginary part of the impedance increased with time irrespective of the type of SS or the processing method. This was observed both in the case of polishing only and conducting pre-immersion and is speculated to be the general behavior of SS in sub-tap water.
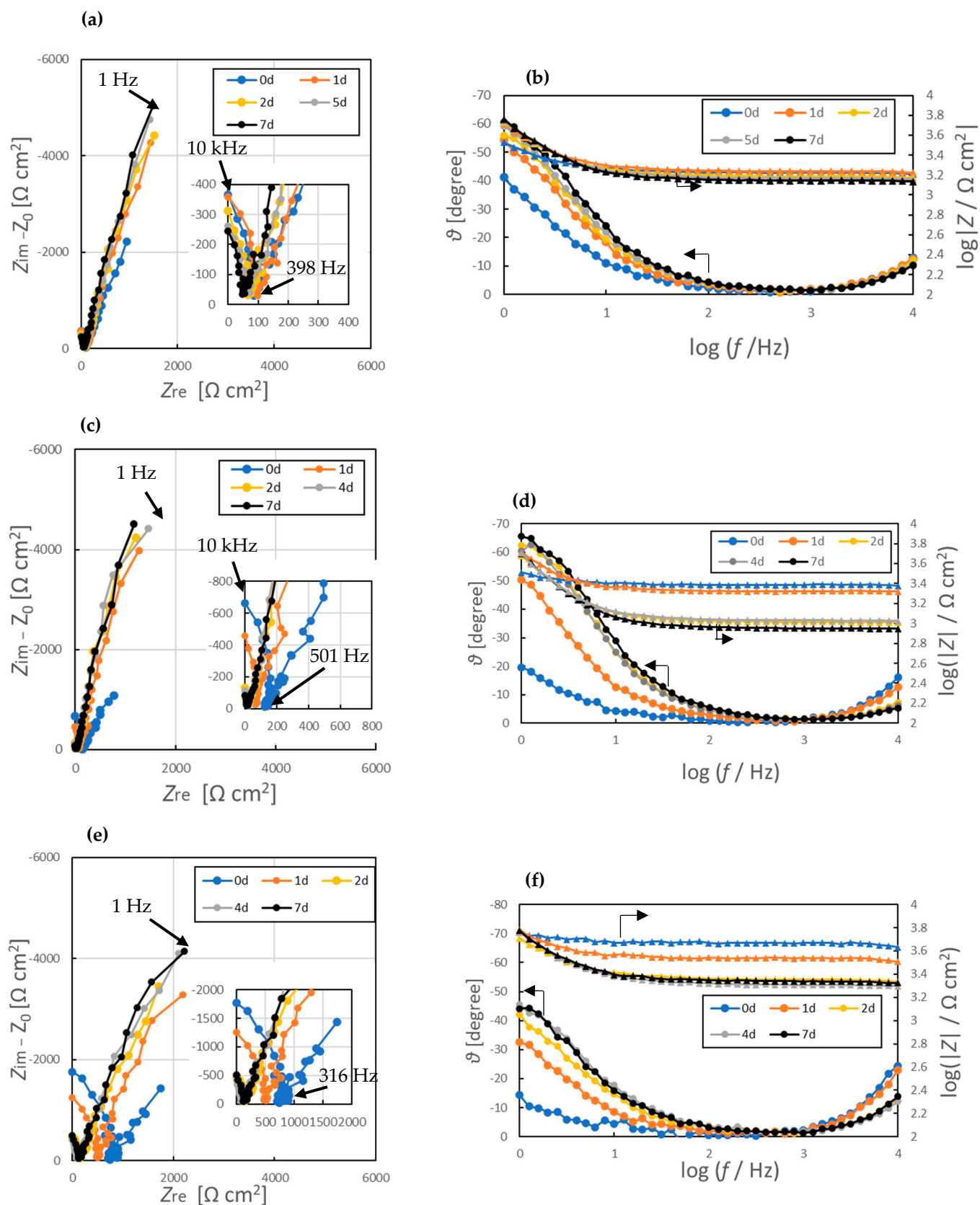
Figure 9. Nyquist diagrams (**a**,**c**,**e**) and Bode diagrams (**b**,**d**,**f**) of EIS spectra for SUS430 subjected to pre-immersion processing for different times: (**a**,**b**) No pre-immersion processing; (**c**,**d**) after immersion in 1 wt% H_2SO_4 solution for 5 min; and (**e**,**f**) after immersion in 1 wt% Na_2CO_3 solution. The circular plots indicate the phase difference, while the triangular plots indicate |Z|.

Comparing the results in the Nyquist diagrams reveals that the change in the surface state of SS strongly affects the stability of the corrosion potential, as indicated by a smaller change in the phase difference over time corresponding to a smaller fluctuation in potential. We therefore speculate that a correlation exists between the time-dependent change in potential and the phase difference obtained by EIS measurements (Figure 10). This trend was also observed when the pretreatment method was changed (Figure S4). In addition, the change in the phase difference is speculated to reflect the change in the surface state because the electric double layer and the film are both related to the capacitance of SS in an aqueous solution. Furthermore, the shape of the curves immediately after the electrodes were immersed in sub-tap water was different, confirming that the surface state could be changed by pre-immersion. This similar tendency was observed for SS samples other than SUS316 (Figures S1–S3).
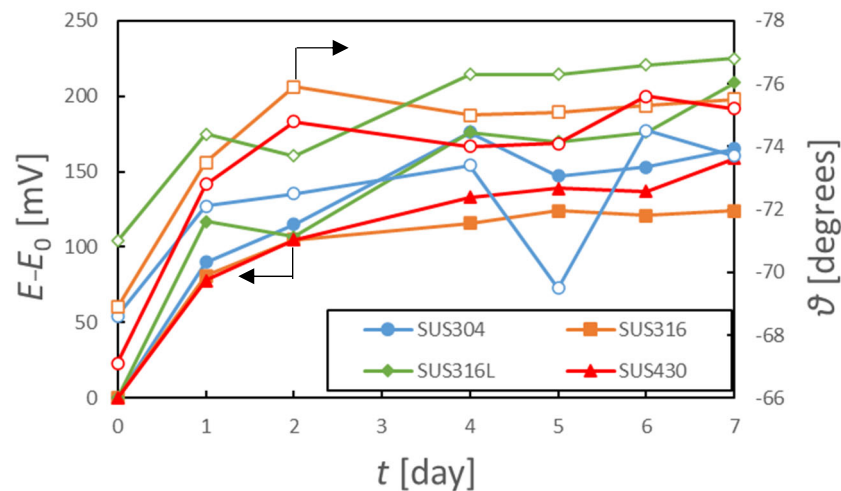

Figure 10. Relationships between potential changes and minimum phase differences of each SS without pretreatment in sub-tap water. The filled plots correspond to the potential, and the hollow plots correspond to the phase.

We also observed that the length of the curve in the imaginary part changed after the electrodes were immersed in sub-tap water; however, this change was not observed for SUS316, and no relationship was found between the length of the curve and the behavior of the potential.

The EIS measurement results were fitted using the equivalent circuit shown in Figure 11, which has been previously proposed to describe the surface state of SS with a passivation film and is particularly applicable to systems with local defects in the film [33–35]. From the result of corrosion potential measurement and polarization, it is considered that the samples also formed a passive film in sub-tap water. Furthermore, it is considered that local defects in the film have appeared because of chlorine in sub-tap water, especially for samples that have been immersed for a long time. Therefore, the equivalent circuit shown was applied to the result of EIS measurements. In the present study, the capacitance was calculated using a constant-phase element (CPE), which considers the deviation from ideal behavior because the characteristics of the film and the double-layer capacitance are not uniform. In this paper, CPE is defined as in Equation (5):

$$Z_{CPE} = [(CPE)(j\omega_c)^\alpha]^{-1} \qquad (5)$$

where (CPE) is the apparent capacitance parameter with units of F cm^{-2} s$^{\alpha-1}$, ω is an angular frequency in rad s^{-1}, and the factor α is the parameter that characterizes deviation of the system from ideal capacitive behavior. In the equivalent circuit, R_s represents the

solution resistance, R_1 and CPE_1 represents the resistance and capacitance related to the redox reaction occurring and/or the film surface, respectively, and R_2 and CPE_2 represent the resistance and capacitance related to the charge transfer occurring on the metal surface, respectively [34,35]. An example of the suitability of the equivalent circuit in Figure 11 to simulate the response of the stainless steels can be seen in Figure S5. From Figure S5, it was confirmed that the fitting results shown in Figure 11 matched well with the experimental results. The fit quality to the experimental results can also be described by Chi-squared (χ^2), which is automatically given in the fitting results. The value of χ^2 by using the equivalent circuit in Figure 11 was a maximum of 3.5742×10^{-4}, suggesting that the circuit is a good model describing the near-surface of SS. In fact, it is difficult to find the two capacitive semicircles from the EIS results. However, since the two time constants of SS are overlapped, it is thought that the circuit in Figure 11 could be used to characterize the surface condition of SS [34]. The results of the fitting using the equivalent circuit in Figure 11 are summarized in Table 6. Although not shown in the table, fitting results showed that the solution resistance R_s ranged from 2.2 kΩ cm^2 to 5.8 kΩ cm^2 and that the resistance of sub-tap water was approximately the same as that of tap water [36]. The fitting showed that the changes in R_2, CPE_2, and α_2 related to charge transfer were smaller for SUS304 and SUS316 than for the other types of SS and that SUS304 and SUS316 showed particularly stable potentials after 5 min of pre-immersion in a 1 wt% H$_2$SO$_4$ solution than for those not subjected to pre-immersion. Conversely, in the case of SUS316L, for which pre-immersion in 1 wt% H$_2$SO$_4$ solution did not lead to substantial improvement in potential stability, either R_2 clearly changed significantly, or the equivalent circuit in Figure 11 was inappropriate for describing the surface condition.
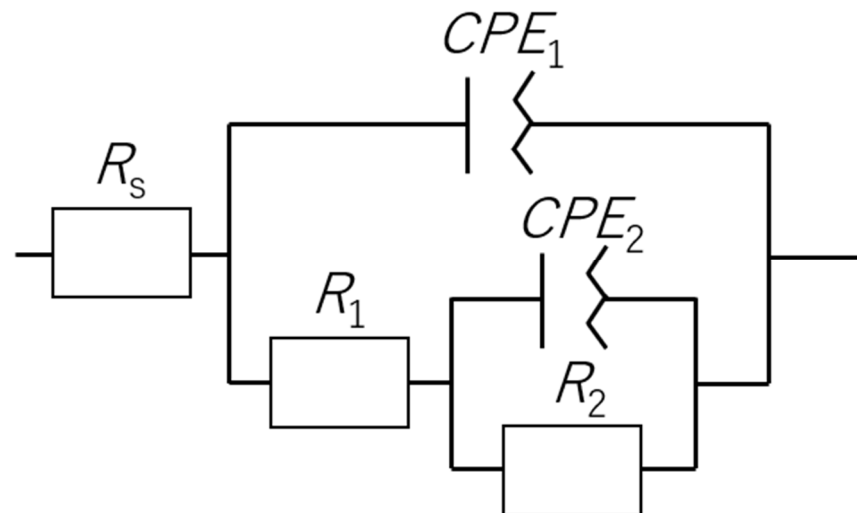

Figure 11. Equivalent circuit to simulate the electrochemical behavior of SS.

Table 6. Parameters calculated from EIS spectra of (**a**) SUS304, (**b**) SUS316, (**c**) SUS316L, and (**d**) SUS430.

Pre-Immersion	Immersion Period [Day]	CPE_1 [μFs$^{\alpha-1}$cm^{-2}]	α_1 [-]	R_1 [kΩcm^2]	CPE_2 [μFs$^{\alpha-1}$cm^{-2}]	α_2 [-]	R_2 [kΩcm^2]	$\chi^2 \times 10^4$ [-]
				(**a**) SUS304				
	0	3.03	0.83	0.28	18.4	0.78	248	0.87
	1	4.91	0.84	1.24	4.82	0.79	178	1.8
N/A	2	8.65	0.81	56.7	0.24	1.00	128	1.3
	5	8.41	0.82	68.0	$\leq 10^{-12}$	1.00	76.1	1.6
	7	7.96	0.82	37.1	$\leq 10^{-12}$	0.16	85.6	1.4

Table 6. *Cont.*

Pre-Immersion	Immersion Period [Day]	CPE_1 [$\mu Fs^{\alpha-1}cm^{-2}$]	α_1 [-]	R_1 [$k\Omega cm^2$]	CPE_2 [$\mu Fs^{\alpha-1}cm^{-2}$]	α_2 [-]	R_2 [$k\Omega cm^2$]	$\chi^2 \times 10^4$ [-]
(a) SUS304								
1% H$_2$SO$_4$ 5 min.	0	21.0	0.87	2.35	17.2	0.78	373	0.96
	1	8.81	0.81	34.8	1.29	1.00	96.3	2.0
	2	8.42	0.81	66.7	0.41	1.00	164	2.4
	4	3.93	0.87	2.25	3.36	0.84	132	1.4
	7	4.11	0.85	2.14	2.63	0.87	137	2.0
1% Na$_2$CO$_3$ 5 min.	0	0.001	1.00	6.73	22.3	0.79	64.1	4.8
	1	13.7	0.73	1.49	7.04	0.86	14.0	0.26
	2	13.8	0.84	203	162	1.00	82.8	0.80
	4	11.7	0.84	193	175	1.00	41.5	0.86
	7	6.55	0.88	1.12	3.26	0.82	166	0.68
30% HNO$_3$ 70 °C 30 min.	0	120.5	0.80	4.16	195.05	1.00	54.3	1.0
	1	35.1	0.87	0.70	14.35	0.89	23.6	1.1
	2	33.8	0.82	1.64	10.42	0.88	33.1	0.50
	5	33.8	0.85	10.7	3.60	1.00	23.2	1.4
	7	38.2	0.98	30.6	21.63	0.84	13.8	3.0
(b) SUS316								
N/A	0	1.23	0.82	0.29	24.6	0.77	359	0.55
	1	10.7	0.85	10.1	1.08	1.00	139	0.54
	2	11.3	0.85	189	93.2	1.00	72.0	1.5
	5	7.60	0.87	2.09	3.13	0.88	155	0.41
	7	10.2	0.85	14.3	6.87	1.00	147	1.1
1% H$_2$SO$_4$ 5 min.	0	26.9	0.78	4.44	9.17	1.00	94.3	0.91
	1	7.82	0.86	1.71	5.33	0.89	375	0.75
	2	6.37	0.91	2.18	4.69	0.91	147	0.71
	5	10.9	0.88	0.56	5.18	0.89	178	0.69
	7	4.57	0.94	0.56	5.31	0.89	148	0.38
1% Na$_2$CO$_3$ 5 min.	0	24.9	0.86	5.74	10.7	1.00	202	1.5
	1	15.5	0.81	113	6.78	1.00	300	1.0
	2	7.13	0.85	12.9	5.23	0.81	95.6	0.28
	4	6.68	0.85	1.23	4.98	0.79	100	0.58
	7	11.9	0.81	11.0	15.0	1.00	174	1.5
30% HNO$_3$ 70 °C 30 min.	0	127	0.69	0.70	71.7	0.87	681.2	1.0
	1	48.1	0.84	1.92	3.52	1.00	17.1	0.77
	2	44.9	0.85	1.24	41.3	0.87	23.6	0.63
	5	39.2	0.87	2.10	3.46	1.00	12.8	0.54
	7	28.0	0.89	0.58	12.1	0.87	26.7	0.65
(c) SUS316L								
N/A	0	87.7	0.71	4.78×10^5	184	0.01	0.010	0.23
	1	30.7	0.83	58.7	255	0.00	65.6	2.1
	2	22.1	0.84	1.25	7.89	0.88	115	1.5
	5	27.7	0.85	226	83.6	0.00	106	2.1
	7	27.4	0.85	314	0.00	1.00	70.3	1.9
1% H$_2$SO$_4$ 5 min.	0	33.6	0.71	3.88	4.76	1.00	22.7	2.0
	1	8.81	0.72	1.39	4.71	0.89	1.34×10^{10}	2.6
	2	9.01	0.86	24.3	0.51	1.00	22.7	1.1
	5	8.13	0.86	2.91	1.00	1.00	248	1.9
	7	4.43	0.93	0.84	3.70	0.87	145	0.47
1% Na$_2$CO$_3$ 5 min.	0	17.2	0.70	4.91	6.30	0.82	151	2.6
	1	11.4	0.78	121	4.63	1.00	241	2.2
	2	8.12	0.83	20.4	0.51	1.00	108	1.6
	4	8.48	0.83	39.8	0.30	1.00	139	1.3
	7	5.42	0.81	3.56	3.11	0.87	175	1.1

Table 6. *Cont.*

Pre-Immersion	Immersion Period [Day]	CPE_1 [$\mu Fs^{\alpha-1}cm^{-2}$]	α_1 [-]	R_1 [$k\Omega cm^2$]	CPE_2 [$\mu Fs^{\alpha-1}cm^{-2}$]	α_2 [-]	R_2 [$k\Omega cm^2$]	$\chi^2 \times 10^4$ [-]
				(**c**) SUS316L				
30% HNO$_3$ 70 °C 30 min.	0	97.2	0.12	1.34	40.3	0.85	1238	15
	1	36.4	0.87	60.0	0.49	1.00	32.3	6.2
	2	33.9	0.89	20.6	1.38	1.00	24.9	2.4
	5	19.8	0.92	0.31	9.54	0.92	37.6	0.46
	7	22.4	0.89	0.61	6.08	0.97	39.9	0.72
				(**d**) SUS430				
N/A	0	28.9	0.79	16.7	2.14	1.00	134	0.79
	1	10.1	0.88	4.04	3.79	0.92	113	0.79
	2	12.0	0.89	35.9	1.65	1.00	69.2	1.7
	5	9.64	0.93	28.3	2.50	1.00	45.8	1.5
	7	11.3	0.87	57.1	0.76	1.00	91.5	2.1
1% H$_2$SO$_4$ 5 min.	0	4.16	0.76	2.43	10.2	0.88	25.1	0.83
	1	13.7	0.85	40.1	0.39	1.00	358	1.2
	2	10.9	0.88	5.17	1.26	1.00	185	0.85
	5	6.56	0.95	1.56	4.47	0.92	104	1.2
	7	11.5	0.89	10.4	0.61	1.00	219	0.58
1% Na$_2$CO$_3$ 5 min.	0	0.004	1.00	4.96	45.6	0.71	30.7	3.2
	1	0.001	1.00	7.67	14.8	0.86	57.8	3.4
	2	7.91	0.40	1.29	13.6	0.79	5.46×10^8	0.92
	4	1.63	0.81	0.49	12.1	0.79	124	0.90
	7	1.23	0.80	0.51	11.9	0.81	121	1.2
30% HNO$_3$ 70 °C 30 min.	0	149.1	0.66	13.4	4.10	1.00	27.5	0.56
	1	91.5	0.69	60.6	71.02	1.00	31.1	1.0
	2	62.9	0.72	3.23	4.95	1.00	16.9	1.2
	5	54.7	0.77	10.5	1.70	1.00	12.4	0.88
	7	52.7	0.77	2.91	2.65	1.00	24.8	0.81

The reaction that strongly affects the potential fluctuation of ~10 mV is thought to be the oxidation of the metal in the bulk part of the SS, which is mainly Fe, to form an oxide film. We assumed that, as the metal ratio of the bulk approaches that of the film, the driving force for supplying the metal to the film decreases, slowing the oxidation reaction on the surface and stabilizing the potential. Bautista et al. [34] have reported that R_2 corresponds mainly to the oxidation reaction from Fe^0 to Fe^{2+}. The Bode plots obtained via the EIS measurements in the present study, including the simulation results for the Bode plot, were similar in shape to those reported by Bautista et al. [34]. Therefore, we speculate that a similar reaction occurred on the sample in the present study and that the oxidation reaction of Fe strongly influences the potential fluctuation.

The state where the potential becomes stable is substantially maintained when the formation of a stable film in a dilute solution is completed, and infinitesimal reactions for keeping the characteristics of the film constant, which corresponds to passive current, mainly continue to progress on the surface. The fitting results show that, in most cases, R_2 was at least 100 times greater than R_1. In a mixed electrode reaction system, the polarization resistance R_p is proportional to the inverse of the corrosion current i_{corr}; however, in this case, the corrosion current was determined by R_2. When the potential stabilized in the sub-tap water, R_2 increased with increasing immersion time, irrespective of the type of SS, and the value converged to ~200 kΩcm^2. This result also shows that the oxidation reaction slowed when the potential stabilized.

The fact that R_2 was large when the potential was stabilized also shows that, when stabilizing the potential of SS, reducing the charge transfer resistance (polarization resistance), as in the case of existing reference electrodes, is not necessary. When focusing on the results after pre-immersion in a 30% HNO$_3$ solution at 70 °C, where the corrosion potential stability deteriorated, R_1 fluctuated by more than one order of magnitude even 2 days

after the electrode was immersed in sub-tap water. Compared with the CPE_1 value for SS electrodes subjected to other treatments, that for the electrode pre-immersed in 30% HNO_3 solution at 70 °C was one order of magnitude larger. From these results, immersion in a 30% HNO_3 solution facilitates the formation of a thin passivation film. The CPE_1 values for samples with stable potentials ranged from 1 to 10 $\mu Fs^{\alpha-1}cm^{-2}$.

5. Conclusions

To develop a QRE that can maintain a stable potential even in dilute solutions and is suitable for use in electrochemical sensors, we evaluated the corrosion potential stability of four types of SSs. It was found that the potential stability is influenced by the corrosion resistance of the material. Among SSs, SUS316 was found to have a standard deviation that was up to 65% smaller even in an untreated state and was found to have the potential to be an excellent material that exhibits a stable potential. As for pre-immersion treatment, it was also found that pre-immersion in 1% H_2SO_4 can reduce the standard deviation by up to 84%, significantly stabilizing the potential of SS.

Polarization tests and EIS measurements revealed that the potential stabilization effect was greatly influenced by oxidation of the bulk metal to form a passivation film, particularly an iron oxide film. We speculated that the potential stability can be further improved by pre-immersing the film to achieve a composition ratio similar to that of bulk steel. No correlation was found between the corrosion resistance of the SS and the corrosion potential stability in the present study.

By comparing the results of analyses conducted using equivalent circuits for SS electrodes with and without passivation, we observed that the film had a sufficient thickness and that growth had stopped when the potential was stabilized. In addition, as the potential stabilizes, the magnitude of the CPE decreases, which suggests that, by manipulating the composition through treatment and carrying out pre-immersion such as etching to smooth the surface, SS electrodes with sufficient potential stability to be used as QREs can be attained.

The corrosion potential stability of SS stabilized by treatment approached that of practical metals such as Cu and Fe. We expect that, in the future, the development of an all-solid-state QRE using SS will lead to the realization of a low-cost, low-energy sensor that can constantly monitor corrosion.

References

1. Bilbao, E.; Garate, O.; Campos, T.R.; Roberti, M.; Mass, M.; Lozano, A.; Longinotti, G.; Monsalve, L.; Ybarra, G. Electrochemical Sweat Sensors. *Chemosensors* **2023**, *11*, 244. [CrossRef]

2. Gross, P.-A.; Larsen, T.; Loizeau, F.; Jaramillo, T.; Spitzer, D.; Pruitt, B. Microfabricated electrochemical gas sensor. *Micro Nano Lett.* **2017**, *11*, 798–802. [CrossRef]

3. Wang, C.; Yang, J.; Li, J.; Luo, C.; Xu, X.; Qian, F. Solid-state electrochemical hydrogen sensors: A review. *Int. J. Hydrogen Energy* **2023**, *48*, 31377–31391. [CrossRef]

4. Xia, D.-H.; Wang, H.-H.; Wang, K.; Fu, C.-W.; Wang, J.-H. A novel electrochemical noise sensor applied to detect food safety. *Russ. J. Electrochem.* **2014**, *50*, 599–602. [CrossRef]

5. Wei, Y.; Hsueh, K.F.; Jang, G.-W. Monitoring the chemical polymerization of aniline by open-circuit-potential measurements. *Polymer* **1997**, *35*, 3572–3575. [CrossRef]

6. Jegdić, B.; Dražić, D.M.; Popić, J.P. Open circuit potentials of metallic chromium and austenitic 304 stainless steel in aqueous sulphuric acid solution and the influence of chloride ions on them. *Corros. Sci.* **2008**, *50*, 1235–1244. [CrossRef]

7. Araneda, A.A.B.; Kappes, M.A.; Rodríguez, M.A.; Ricardo, M. Carranza Pitting corrosion of Ni-Cr-Fe alloys at open circuit potential in chloride plus thiosulfate solutions. *Corros. Sci.* **2022**, *198*, 110121. [CrossRef]

8. Wilburn, J.P.; Ciobanu, M. Characterization of Acrylic Hydrogels by Open Circuit Potential Monitoring. *J. Appl. Electrochem.* **2004**, *39*, 729–734. [CrossRef]

9. Doménech-Carbó, A.; Ronda, M.A.P.; Vives-Ferrándiz, J.; Duffó, G.S.; Farina, S.; Doménech-Carbó, M.T. Modeling 'dry' OCP measurements to characterize archaeological iron corrosion I: Long-time transients. *J. Electroanal. Chem.* **2022**, *913*, 116210. [CrossRef]

10. Probst, D.; Lee, I.; Sode, K. The development of micro–sized enzyme sensor based on direct electron transfer type open circuit potential sensing principle. *Electrochem. Acta* **2022**, *426*, 140798. [CrossRef]

11. Ghilane, J.; Hapiot, P.; Bard, A.J. Metal/Polypyrrole Quasi-Reference Electrode for Voltammetry in Nonaqueous and Aqueous Solutions. *Anal. Chem.* **2006**, *78*, 6868–6872. [CrossRef]

12. Kasem, K.K.; Jones, S. Platinum as a reference electrode in electrochemical measurements. *Platinum Met. Rev.* **2008**, *52*, 100–106. [CrossRef]

13. Dawkins, R.C.; Wen, D.; Hart, J.N.; Vepsäläinen, M. A screen-printed Ag/AgCl reference electrode with long-term stability for electroanalytical applications. *Electrochem. Acta* **2021**, *393*, 139043. [CrossRef]

14. Arioka, S.; Matsuoka, M.; Yamamoto, T.; Komori, K.; Inoue, H. The Condition Monitoring of a Chemical Plant with the On-Line Measurement of Corrosion Potential Variation and Corrosion Potential Noise. *Zair.-Kankyo* **2014**, *63*, 600–608. [CrossRef]

15. Andriukonis, E.; Butkevicius, M.; Simonis, P.; Ramanavicius, A. Development of a Disposable Polyacrylamide Hydrogel-Based Semipermeable Membrane for Micro Ag/AgCl Reference Electrode. *Sensors* **2023**, *25*, 2510. [CrossRef] [PubMed]

16. Torres-González, V.; Ávila-Niño, J.A.; Araujo, E. Facile fabrication of tailorable Ag/AgCl reference electrodes for planar devices. *Thin Solid Film.* **2022**, *757*, 139413. [CrossRef]

17. Manjakkal, L.; Vilouras, A.; Dahiya, R. Screen Printed Thick Film Reference Electrodes for Electrochemical Sensing. *IEEE Sens. J.* **2018**, *18*, 7779–7785. [CrossRef]

18. Auer, A.; Kunze-Liebhäuser, J. A universal quasi-reference electrode for in situ EC-STM. *Electrochem. Commun.* **2019**, *98*, 15–18. [CrossRef]

19. Truong, T.N.P.; Randriamahazaka, H.; Ghilane, J. Platinum/poly(N-ferrocenylmethyl-N-allylimidazolium bromide) quasi-reference electrode for electrochemistry in non-aqueous and ionic liquid solutions. *Electrochem. Commun.* **2016**, *73*, 5–9. [CrossRef]

20. Keeble, L.; Jaccottet, A.; Ma, D.; Rodriguez-Manzano, J.; Georgiou, P. An electroplated Ag/AgCl quasi-reference electrode based on CMOS top-metal for electrochemical sensing. *Electrochem. Acta* **2024**, *477*, 143780. [CrossRef]

21. Lee, J.; Jäckel, N.; Kim, D.; Widmaier, M.; Sathyamoorthi, S.; Srimuk, P.; Kim, C.; Fleischmann, S.; Zeiger, M.; Presser, V. Porous carbon as a quasi-reference electrode in aqueous electrolytes. *Electrochim. Acta* **2016**, *222*, 1800–1805. [CrossRef]

22. Brainina, K.Z.; Tarasov, A.V.; Vidrevich, M.B. Silver Chloride/Ferricyanide-Based Quasi-Reference Electrode for Potentiometric Sensing Applications. *Chemosensors* **2020**, *8*, 15. [CrossRef]

23. Narivskyi, O.E.; Subbotin, S.A.; Pulina, T.V.; Khoma, S. Assessment and Prediction of the Pitting Resistance of Plate-Like Heat Exchangers Made of AISI304 Steel and Operating in Circulating Waters. *Mater. Sci.* **2022**, *58*, 41–46. [CrossRef]

24. Olefjord, I.; Clayton, C.R. Surface Composition of Stainless Steel during Active Dissolution and Passivation. *ISIJ Int.* **1991**, *31*, 134–141. [CrossRef]

25. Mori, Y.; Hashimoto, M.; Liao, J. Effect of Surface Composition on Contact Resistivity and Corrosion Resistance of 316L Stainless Steel. *ISIJ Int.* **2013**, *53*, 1057–1061. [CrossRef]

26. Cui, C.Y.; Cui, X.G.; Ren, X.D.; Qi, M.J.; Hu, J.D.; Wang, Y.M. Surface oxidation phenomenon and mechanism of AISI 304 stainless steel induced by Nd:YAG pulsed laser. *Appl. Surf. Sci.* **2014**, *305*, 817–824. [CrossRef]

27. *JIS G0579*; Method of Anodic Polarization Curves Measurement for Stainless Steels. Japanese Standards Association: Tokyo, Japan, 2007.

28. Takizawa, K. Passivation of Stainless Steel. *J. Surf. Finish. Soc. Jpn* **1990**, *41*, 9–16.

29. Pourbaix, M. *Atlas of Electrochemical Equilibria in Aqueous Solutions*; National Association of Corrosion Engineers: Houston, TX, USA, 1974.

30. Yang, Y.; Wang, Q.; Li, J.; Tan, L.; Yang, K. Enhancing General Corrosion Resistance of Biomedical High Nitrogen Nickel-Free Stainless Steel by Nitric Acid Passivation. *Acta Metall. Sin. (Engl. Lett.)* **2020**, *33*, 307–312. [CrossRef]

31. Guha, H.; Saiers, J.E.; Brooks, S.; Jardine, P.; Jayachandran, K. Chromium transport, oxidation, and adsorption in manganese-coated sand. *J. Contam. Hydrol.* **2001**, *49*, 311–334. [CrossRef]

32. Freire, L.; Catarino, M.A.; Godinho, M.I.; Ferreira, M.J.; Ferreira, M.G.S.; Simões, A.M.P.; Montemor, M.F. Electrochemical and analytical investigation of passive films formed on stainless steels in alkaline media. *Cem. Concr. Compos.* **2012**, *34*, 1075–1081. [CrossRef]

33. Takatoshi, S.; Yoichi, K. The fundamentals of Corrosion of Aluminum IX. *UACJ Tech. Rep.* **2014**, *1*, 82–91.

34. Bautista, A.; González-Centeno, A.; Blanco, G.; Guzmán, S. Application of EIS to the study of corrosion behaviour of sintered ferritic stainless steels before and after high-temperature exposure. *Mater. Charact.* **2008**, *59*, 32–39. [CrossRef]

35. Zheng, Z.J.; Gao, Y.; Gui, Y.; Zhu, M. Studying the fine microstructure of the passive film on nanocrystalline 304 stainless steel by EIS, XPS, and AFM. *J. Solid State Electrochem.* **2014**, *18*, 2201–2210. [CrossRef]

36. Abe, B.-I. Ions in aqueous solutions and electrical conductivity. *Kagaku Kyoiku* **2009**, *52*, 562–565. (In Japanese)